Facile and efficient Cu(0)-mediated radical polymerisation of pentafluorophenyl methacrylate grafting from poly(ethylene terephthalate) film

- Thi Phuong Thu Nguyen, Nadine Barroca-Aubry, Diana Dragoe, Sandra Mazerat, François Brisset, Jean-Marie Herry, Philippe Roger

Facile and efficient Cu(0)-mediated radical polymerisation of pentafluorophenyl methacrylate grafting from poly(ethylene terephthalate) film

*Thi Phuong Thu Nguyen [a], Nadine Barroca-Aubry [a], Diana Dragoe [a], Sandra Mazerat [a], François Brisset[a], Jean-Marie Herry[b], Philippe Roger[a] **

[a] Institut de Chimie Moléculaire et des Matériaux d'Orsay (ICMMO), UMR 8182, Univ. Paris Sud, Université Paris Saclay, 91405, Orsay, France

[b] INRA, AgroParisTech, Université Paris Saclay, UMR 782, GMPA, Ecomic, 1, avenue des Olympiades, Massy F-91300, France

*Corresponding Author: *philippe.roger@u-psud.fr*

Abstract

Grafting polymers bearing active esters, especially pentafluorophenyl methacrylate (PFPMA), onto or from surface is a promising approach towards the preparation of highly functional materials due to the ease in post-polymerisation modification of their corresponding polymers. Herein, a handy and efficient chemical modification process is proposed to modify extreme surface of poly(ethylene terephthalate) (PET) films towards the final purpose of grafting PFPMA polymer from PET surface via surface-initiated Cu(0)-mediated radical polymerisation. The characteristics of modified surface were evaluated after each step using various techniques including water contact angle, attenuated total reflectance Fourier-transform infrared spectroscopy, X-ray photoelectron spectroscopy, atomic force microscopy, and scanning electron spectroscopy. Due to its robust conditions, the proposed approach allows grafting at ease PFPMA polymer from PET supporting surface, which not only enhances the reactivity of this inert material but also improves significantly the hydrophobicity of the surface.

Highlights

- For the first time, poly(pentafluorophenyl methacrylate) was successfully grown from poly(ethylene terephthalate) films *via* surface-initiated Cu(0)-mediated radical polymerisation.
- The use of Cu(0)-mediated radical polymerisation allows a robust reaction condition, while eliminating the time and effort needed to freeze-thaw-pump.
- This approach might be applied on both small scale of 1-2 films and large scale of 12 individual films yet maintaining the full coverage of poly(pentafluorophenyl methacrylate) over supporting surface.
- Obtained surfaces showed an enhancement in hydrophobicity and increase in roughness compared to virgin poly(ethylene terephthalate) films.

Keywords: pentafluorophenyl methacrylate, active ester, poly(ethylene terephthalate), surface-initiated polymerisation, copper mediated polymerisation, surface modification.

1. Introduction

Surface modification, especially in the case of polymer substrates, has been greatly exploited for altering performance and characteristics of materials for a number of applications[1-11]. Among many types of polymers widely used, poly(ethylene terephthalate) (PET) is one of the most popular polyesters as it possesses several advantageous physical properties, such as good mechanical strength, relatively high toughness, high melting temperature, and notably the possibility of recycling[12, 13]. Due to its high resistance in common organic solvents and its low surface energy, a wide range of approaches have been employed to activate the inert PET surface including plasma treatment[14-17], photo/UV irradiation[18-20], and wet chemistry[21-23] to enhance a specified characteristic of the material such as the wettability[24], antimicrobial property[20, 25, 26], biocompatibility[27, 28] and stimuli responsiveness[29, 30]. However, published work on this field is often characterized for one specified type of compound, which might eventually not be replicable for other functional groups. Therefore, there is somewhere the need for a multi-purpose reactive PET surface that could undergo several different subsequent modifications in an extremely convergent way so that one can graft to the supporting

surface at will a specified compound or functional groups. It is possible to fulfil that need by grafting polymer of active esters onto or from PET surfaces, which in consequence, allowing further introduction of new functional groups to a main chain or substrate[31-33]. Among currently known active esters, pentafluorophenyl methacrylate (PFPMA) has been used extensively as its polymer is soluble in a wide range of solvents and could be substituted easily with amines, alcohols[31, 34], or thiols at different molar equivalence[35, 36]. Controlled polymerisation of PFPMA in solution is well studied and widely applied but mainly by radical addition and fragmentation transfer (RAFT) polymerisation[34, 37-39], only limited amount of work has been dedicated to atom transfer radical polymerisation (ATRP) of PFPMA[40, 41]. In contrast, among a few examples in literature regarding surface initiated (SI) polymerisation of PFPMA[37, 42-44], the technique of dominance is SI-ATRP rather than SI-RAFT polymerisation as the later requires chain transfer agent which is frequently tailor-made for a polymerisation condition. However, classical ATRP itself also possesses some disadvantages such as the use of air-sensitive reagents and high dose of copper catalysts which lead to crucial extra work to avoid the presence of air, difficulties in polymer purification and over cost. Several ATRP alternatives like ICAR-ATRP, A(R)GET-ATRP, eATRP, photo-induced ATRP, SARA-ATRP/SET-LRP have been developed to overcome the disadvantages of classic ATRP. Among those, the introduction of zero valent copper in ATRP system, which was firstly introduced in 1997[45], is considered one of the most convenient alternatives to reduce the over dose of catalyst as well as the over workload in avoiding presence of oxygen/air. Regardless of the debate between Supplemental Activation and Reducing Agent (SARA) ATRP and Single Electron Transfer Living Radical Polymerisation (SET-LRP) on the role of Cu(0) in the catalytic mechanism, the use of Cu(0)-mediated radical polymerisation has been successfully used to graft different polymers from several substrates[46-54] . However, to the best of our knowledge, no report is available in literature regarding the employ of this technique for preparing polymer of PFPMA neither in solution nor from any supporting surface. Herein, the use of surface initiated Cu(0)-mediated radical polymerisation is reported as an efficient and handy approach to graft PFPMA polymers from PET surface. This alternative approach not only allows for the graft of PFPMA polymer on small scale but it is also applicable for a larger batch of polymerisation, opening the possibility for its application on industrial scale.

77 ## 2. Materials and Methods

78 ### 2.1. Materials

79 Pentafluorophenol (TCI, 98%), methacryloyl chloride (Sigma-Aldrich, 97%, stabilized), branched
80 polyethyleneimine (PEI) (Sigma Aldrich) (average Mw 25 000 g.mol^{-1}), Orange II dye (TCI, >97%),
81 α-Bromoisobutyryl bromide (BiBB) (Aldrich, 98%), tris(2-pyridylmethyl) amine (TPMA) (TCI, 98%),
82 copper (II) bromide (Aldrich), geraniol (Aldrich, 98%), 1,8-Diazabicyclo[5.4.0]undec-7-ene (DBU)
83 (Sigma-Aldrich, 98%), dimethyl sulfoxide (DMSO) (Fisher Chemicals), tetrahydrofuran (THF) (VWR
84 Chemicals) and sulfolane (TCI) were used as received. Triethylamine (TEA) (Sigma-Aldrich) was
85 distilled over KOH pellets before used. Dimethylformamide (DMF) (VWR Chemicals) was dried with
86 calcium hydride. Melinex® Poly(ethylene terephthalate) films (thickness of 125 μm) were obtained
87 from Pütz-Folien (Germany). Copper(0) annealed wire is product of Alfa Aesar, 1.0 mm in diameter,
88 density of 7.02 g m^{-1}.

89 ### 2.2. Methods

90 #### 2.2.1. Water contact angle measurement

91 Static contact angle measurement was performed using a DSA100 Kruss analyser. The contact angle
92 was measured by depositing a 3 μL droplet of milliQ water on surface, an average contact angle was
93 calculated from 3 droplets for each film, and errors were calculated as standard deviation.

94 Surface homogeneity wettability was investigated by water contact angle measurements using the
95 sessile drop technique with a micro-goniometer (DSA100 M, Krüss, Les Ulis, France). This device
96 deposited a deionized water droplet (300 pL) with a piezo dosing unit every 1 mm on a rectangular
97 zone of 20 mm × 10 mm. Droplets were monitored for 2 s with a fast CCD camera with 4× zoom and a
98 20× microscope objective. The angle of interest was the one obtained on the first acquisition image
99 because of the very quick evaporation process of the small drops. The water contact angle and standard
100 deviation were calculated as average of all captured droplets deposited on surface.

101 **2.2.2. UV-Vis measurement**

102 UV-Vis absorbance determination was carried out with Varian Cary 1E UV-Visible spectrometer
103 using two-sided disposable 3-mL VWR® polystyrene cuvettes with light path of 10 mm.

104 **2.2.3. Attenuated Total Reflectance (ATR) FTIR**

105 Absorbance of films was measured by Bruker IFS 66 equipment with an ATR module using diamond
106 crystals of Pike technologies. 200 scans of resolution 4 cm^{-1} were recorded between 600 cm^{-1} to 4000
107 cm^{-1}. Spectra visualization and treatment were done using OPUS software; spectra integration was
108 done using the built-in integration function of Origin® v8.0724.

109 **2.2.4. X-ray Photoelectron Spectroscopy (XPS)**

110 K-alpha spectrometer from ThermoFisher, equipped with a monochromatic X-ray source (Al K-alpha,
111 1486.6 eV). A spot size of 400 mm was employed; the hemispherical analyser was operated in CAE
112 (Constant Analyzer Energy) mode, with passing energy of 200 eV, a step of 1 eV for the acquisition of
113 survey spectra, and 50 eV and 0.2 eV for high resolution spectra. A "dual beam" flood gun was used to
114 neutralize the charge build-up. The obtained spectra were treated by CasaXPS® version 2.3.19. A
115 Shirley-type background subtraction was used and the peak areas were normalized using the Scofield
116 sensitivity factors in the calculation of elemental compositions. Fitting was carried out by calibrating
117 binding energy of C=C peak to 284.8 eV or binding energy of C-C peak to 285 eV. All lineshapes
118 were considered to be a 30/70 or 40/60 mix of Gaussian and Lorentzian distributions.

119 **2.2.5.Atomic Force Microscopy (AFM)**

120 Tapping mode topography and phase imaging was accomplished using di Innova AFM Bruker with
121 NanoDrive v8.02 software. Tapping mode images were acquired using silicon tips from Nanosensors
122 (PPP NCSTR) with a resonance frequency ranging between 76 and 263 kHz. Image processing was
123 performed and visualized using WSxM software[55].RMS indicates root-mean-square roughness of
124 obtained at focusing window of 10μm x 10μm.

125 **2.2.6. Scanning Electron Microscopy (SEM)**

126 Scanning Electron Microscopy (SEM) was performed at short working distance using a field emission
127 gun (FEG) at low voltage (1 kV) and low current (few pA) in order to observe only the extreme
128 surface of sample, hence, allowing the comparison with AFM images.

129 ## 3. Experimental

130 **3.1.1. Synthesis of pentafluorophenyl methacrylate (PFPMA)**

131 Pentafluorophenol (25 g, 0.135 mol) was dissolved in 300 mL of anhydrous dichloromethane.
132 Triethylamine (21 mL, 0.151 mol) and methacryloyl chloride (12 mL, 0.125 mol) were successively
133 introduced via a tight Ar-washed syringe at 0 ºC. Reaction mixture was stirred for 3 hours at 0 ºC then
134 left stirring overnight at room temperature. Reaction mixture was then filtered, the filtrate was washed
135 with distilled water and saturated aqueous K_2CO_3 solution several times. The collected organic phase
136 was then dried over anhydrous $MgSO_4$ and purified by distillation under vacuum at 85 ºC to collect
137 transparent, colourless liquid. Yield: 80%. ^{1}H-NMR (250 MHz, $CDCl_3$, ppm): δ 2.06 (s, 3H, $-CH_3$),
138 5.89 (s, 1H, $=CH_2$), 6.43 (s, 1H, =CH-). ^{19}F-NMR (250 MHz, $CDCl_3$, ppm): δ -162.45 (t, 2F, meta
139 positions), -158.14 (t, 1F, para position), -152.75 (d, 2F, ortho positions).

140 **3.1.2.Preparation of PET-NH_2 film by aminolysis**

141 PET films of 1 cm x 2 cm were cleaned with EtOH:H_2O (1:1 vol.) by shaking for 15 minutes then
142 washed with acetone and dried under vacuum. Dry films were immersed in a solution of PEI 5% (w/w)
143 in DMSO in a 50 ºC preheated water bath. After 6 hours, films were washed with excess DMSO by
144 shaking at 200 rpm overnight. Films were then cleaned with excess deionized water until no
145 absorption under UV light at 214 nm was detected, indicating the complete removal of non-specific
146 attached PEI and DMSO. Finally, films were subsequently rinsed with acetone and dried under
147 vacuum at room temperature.

148 **3.1.3. UV-Vis titration of amino groups by orange II dye**

149 The titration of amino groups on PET surface was done as described in literature by the use of orange
150 II dye [56]. Briefly, each film was immersed in 2 mL of orange II dye in acidic water (pH 3, dye
151 concentration 15 $mg.mL^{-1}$) for 45 minutes at 40 ºC. Non-specific interaction dye was removed by
152 subsequently washing films in acidic water (pH 3). Detachment of adsorbed dye was performed by
153 dipping films in basic water (pH 12) for a few minutes, solution of detached dyes was adjusted to pH 3
154 using concentrated HCl. Absorbance was measured between 350 - 600 nm, maximum absorbance at
155 484 nm was recorded and the amount of amino groups was reported as number of group per nm^2.

156 A calibration curve was obtained using Orange II dye solution in acidic water (pH 3) at several dye
157 concentrations of $9x10^{-4}$, $18x10^{-4}$, $27x10^{-4}$, $36x10^{-4}$ and $72x10^{-4}$ $mg.mL^{-1}$ to obtain the wavelength-
158 dependent molar absorptivity coefficient (ε) of 51.3 $M^{-1}cm^{-1}$.

159 **3.1.4. Immobilisation of initiator (PET-Br films)**

160 2 films were placed face-to-face in a special designed mini reactor. In a pear-shaped flask, 6 mini-
161 reactors (12 films) were placed vertically. The reactor was purged with a strong argon stream, and then
162 35 mL of anhydrous diethylether was introduced via an air-tight syringe. 5 mL of triethylamine (0.036
163 mmol) was injected at 0 ºC, followed by 3.75 mL of α-bromoisobutyryl bromide (0.03 mmol)
164 dropwise. The reaction was kept at 0 ºC for 3 hours, and then left overnight at room temperature. Films
165 were removed from solution and washed several times with excess amount of dichloromethane,
166 acetone and water then dried under vacuum.

167 **3.1.5. Surface-initiated Cu(0)-mediated radical polymerisation of PFPMA**

168 For surface of **PET-*g*-PFPMA-110** and **PET-*g*-PFPMA-127**: in a modified 10 mL round-bottom vial,
169 2 films were placed face-to-face, then 2 mL of DMSO:Sulfolane (1:4 vol.) containing 3.5 mg of
170 TPMA and 0.8 mg of $CuBr_2$ was injected via an air-tight syringe. Reactor was then purged with a
171 mediate argon stream for 5 minutes, then 660 μL of PFPMA (3.4 mmol) and a prewashed U-shaped
172 Cu(0) wire were introduced (total 2.5 cm). The reactor was then capped, sealed with parafilm and
173 placed in a 60 ºC preheated oil bath for 24 hours (PET-*g*-PFPMA-110) and 72 hours (PET-*g*-PFPMA-

127). Films were removed from solution and washed with excess amount of dichloromethane, acetone and water several times, then dried and stored under vacuum prior to analysis.

Large batch reaction (**PET-*g*-PFPMA-90**): 43.0 mg of TPMA (0.148 mmol) and 8.0 mg of $CuBr_2$ (0.036 mmol) were dissolved in a mixture of 6 mL DMSO and 24 mL sulfolane in a 50 mL eggplant-shaped flask. 12 films in 6 mini-reactors were then arranged vertically in the flask, each mini-reactor also contained a U-shaped Cu^0 wire of 5 cm. 5 mL of PFPMA (22.03 mmol) was injected via an air-tight syringe. The flask was then purged with a modest flow of argon for 15 minutes. The reaction was carried out in a 60 ^oC preheated oil bath for 24 hours. Films were then washed with excess amount of dichloromethane, acetone and water several times, then dried and stored under vacuum prior to analysis.

3.1.6. Post-modification of PET-*g*-PFPMA-90 films with geraniol

12 films were placed in 6 mini-reactors as used in large batch polymerization. Anhydrous DMF was introduced under a moderate stream of argon, then 1.2 mL of geraniol (6.9 mmol) and 400 μL of DBU (2.7 mmol) were adjusted via air-tight syringe. The reaction flask was placed in a preheat oil bath at 50^oC for 24 hours. Films were then immersed in clean THF with shaking at 200 rpm overnight to removed excess DMF and DBU physically adsorbed onto surface. After that, PET-GeMA films were washed with copious amount of methanol, distilled water, acetone then dried under reduced pressure.

4. Results and Discussion

The PET film surface was modified as presented in

Scheme 1 by aminolysis, followed by initiator immobilisation and then surface-initiated polymerisation mediated by Cu(0) of PFPMA. After each modification, surface was characterised by different analysis techniques including water contact angle to quickly access changes occurred on extreme surface of materials, ATR FTIR to give an approximation of the chemical function present on surface, XPS to quantify atomic percentage of elements appeared on surface, and finally AFM in parallel with SEM to visualise the topography of surface.

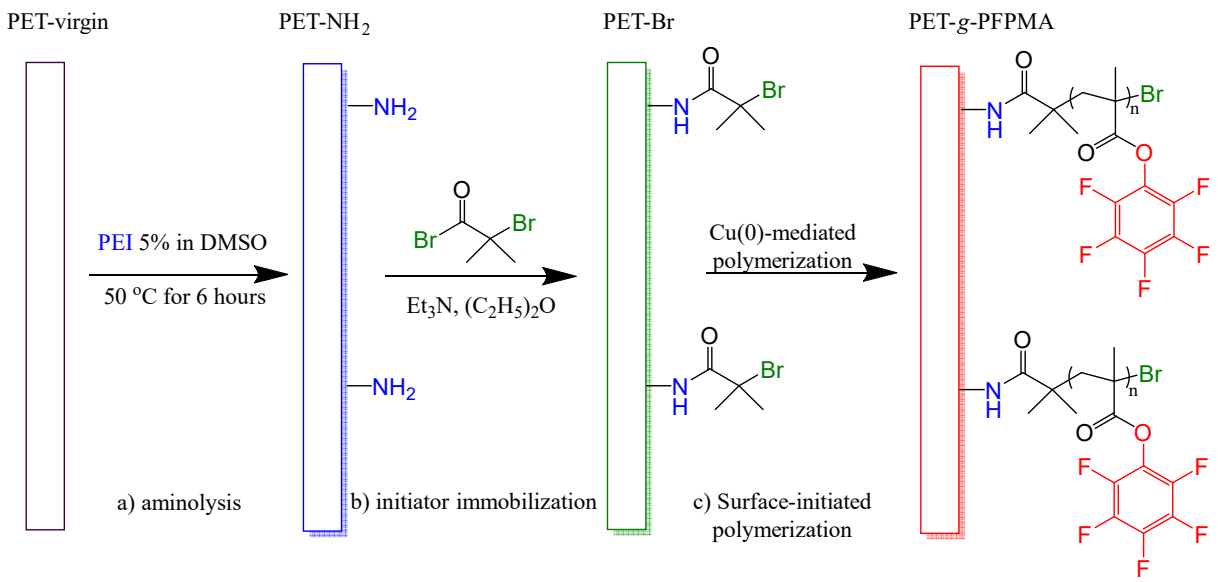

Scheme 1. General scheme of surface-initiated polymerisation mediated by Cu(0) to graft polymer of PFPMA from PET surfaces.

4.1. Quantification of amino groups before/after aminolysis and initiator immobilisation

To graft polymers onto or from PET surface using wet chemistry, several approaches have been presented to activate the inert surface by generating either hydroxyl groups via the hydrolysis of the surface [15, 57, 58] or amino groups by aminolysis with amines [22, 59]. Herein, PET surface was activated by aminolysis of the surface using PEI 5% solution in DMSO at 50°C for 6 hours. As shown in Figure 1, titration of amino functional group on surface with orange II dye of virgin (clean, non-modified) PET surface showed very low presence of amino group on the surface. In contrast, the amount of amino groups on PET-NH_2 surface increased to 0.61 ± 0.04 NH_2 per nm^2 after aminolysis, which showed good agreement with results reported previously by our group[30] employing the same approach.

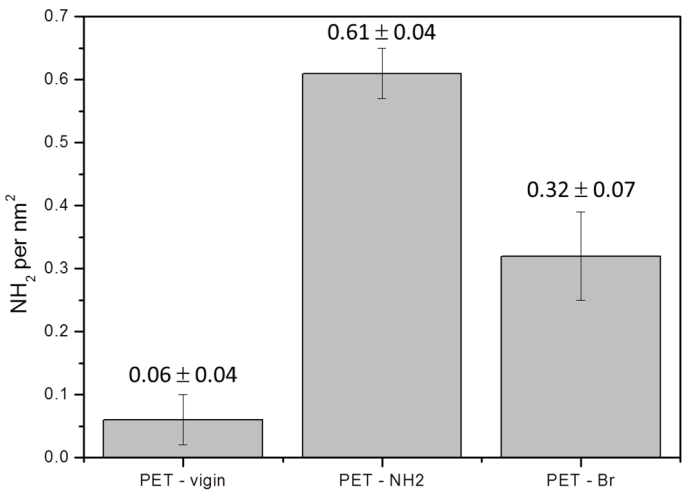

Figure 1. Orange II dye titration: amine quantification on PET-virgin, PET-NH_2 and PET-Br

Bromoisobutyryl initiator was then immobilized onto the surface through the reaction between amines and α-bromoisobutyryl bromide (BiBB). Titration with orange II dye was repeated in order to estimate the amount of remaining amine, and therefore, indirectly determine the yield of initiator immobilisation. The results of 0.32 ± 0.07 NH_2 per nm^2 indicates that around 0.3 NH_2 per nm^2 have reacted with BiBB, corresponding to an initiator density of 0.3 groups per nm^2. Therefore, the density of tethered polymer grafting from such initiator is expected to be 0.3 chains per nm^2. Furthermore, the grafting density of 0.3 chains per nm^2 corresponds to chains in high density brush regime as reported in literature[60, 61] suggesting a complete coverage of the active polymer.

4.2. The change in extreme surface measured by water contact angle

Surface modification results in an enormous change in chemical properties of extreme outer layer of materials, hence, the static water contact angle has been used as the first and fastest method to verify the success of a modification technique. As seen in Figure 2 (a, b, c), virgin PET film became more hydrophilic after aminolysis with PEI due to the appearance of amino groups on the surface, which subsequently led to the drop in water contact angle from $82^o \pm 2$ to $55^o \pm 5$. After initiator introduction, the water contact angle rose to $67^o \pm 3$, suggesting the presence of methyl groups and bromine atoms, which are less polar compared to amino groups.

229 Surface-initiated Cu(0)-mediated radical polymerisation of PFPMA from PET-Br surface was done in
230 DMSO:sulfolane (1:4 in volume) mixture with molar feed ratio among reactants of
231 $[PFPMA]_0/[TPMA]_0/[CuBr_2]_0$ = 612/4/1 for large batch and $[PFPMA]_0/[TPMA]_0/[CuBr_2]_0$ = 944/4/1
232 for small batch and a Cu(0) wire of certain length. It is worth to note that the amount of grafted
233 initiator is very small to the amount of monomer; hence, one might not expect a good control in this
234 surface-initiated polymerisation system.

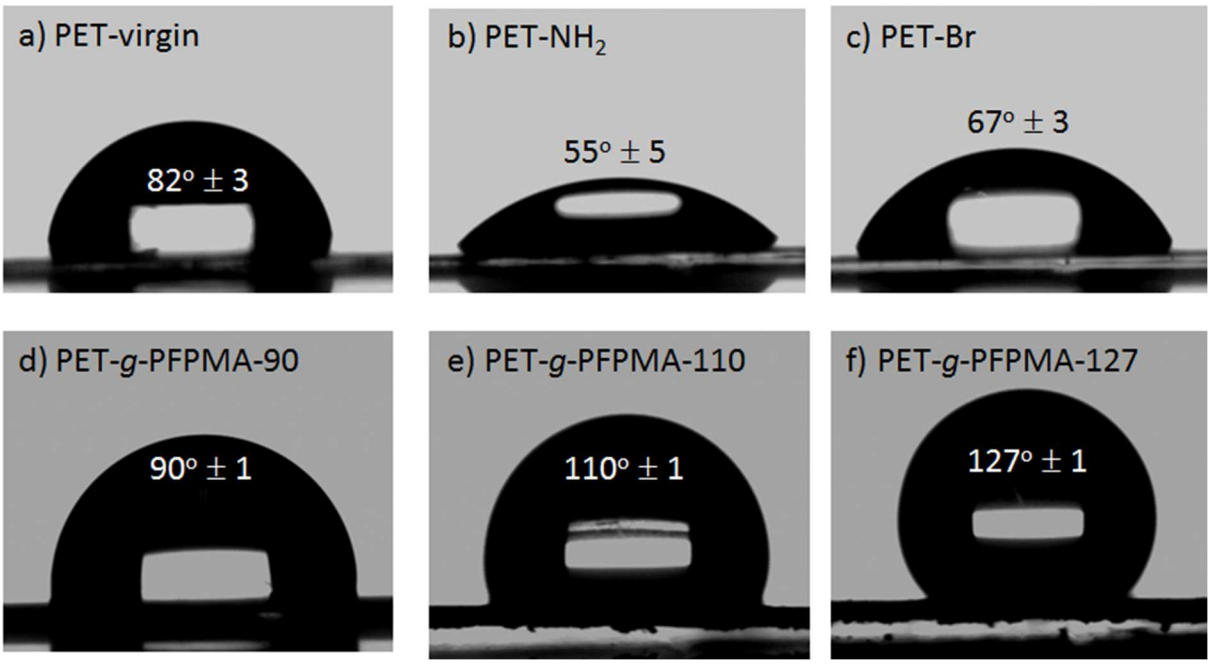

235

236 **Figure 2. Water contact angle of PET surface after each polymerisation: a) virgin PET, b) PET**
237 **after aminolysis (PET-NH_2), c) PET after immobilisation of initiator (PET-Br), d) PET grafted**
238 **with PFPMA after large batch polymerisation (PET-*g*-PFPMA-90), e) PET grafted with PFPMA**
239 **after 1-day small batch polymerisation (PET-*g*-PFPMA-110), f) PET grafted with PFPMA after**
240 **3-day small batch polymerisation (PET-*g*-PFPMA-127).**

241 As predicted, the presence of nonpolar moieties on extreme surface of PET after polymerisation has
242 led to an increase in water contact angle from 67° of PET-Br surface to 110° (1-day polymerisation),
243 reaching 127° (3-day polymerisation), higher than those observed in literature from SI-RAFT
244 polymerisation[37]. When a lower degree of polymerisation is expected (in the case of large batch
245 condition), the contact angle still reaches 90° after 24 hours, which is the minimum threshold between
246 hydrophilic and hydrophobic surface classification.

As the large batch polymerisation of 12 films allows the preparation of several films at the same time, it is of our interest to investigate the homogeneity of the surface obtained by this approach. Therefore, a study on water contact angle of PET-virgin and PET-*g*-PFPMA-90 films by micro-goniometer was done by depositing 231 water droplets of 300-picolitre on the 1 cm x 2 cm film. It is noted that there is a few degree difference in results between conventional contact angle and micro-goniometer due to the huge difference not only in volume of droplet but also in the evaporation rate. Figure 3 presents the photos of 56 droplets deposited in the centre region of PET-virgin and PET-*g*-PFPMA-90 films. It is seen that the PET-*g*-PFPMA-90 surface has a comparable homogeneity with the non-modified surface. Furthermore, water contact angles of all drops on surface (Supporting Information, Figure S2) presents to be identical with a difference of 2-3 degree in WCA. This result indicates that the surface-modification process as well as the surface-initiated polymerisation has proceeded in a uniform manner and the polymer of PFPMA has completely covered the supporting surface.

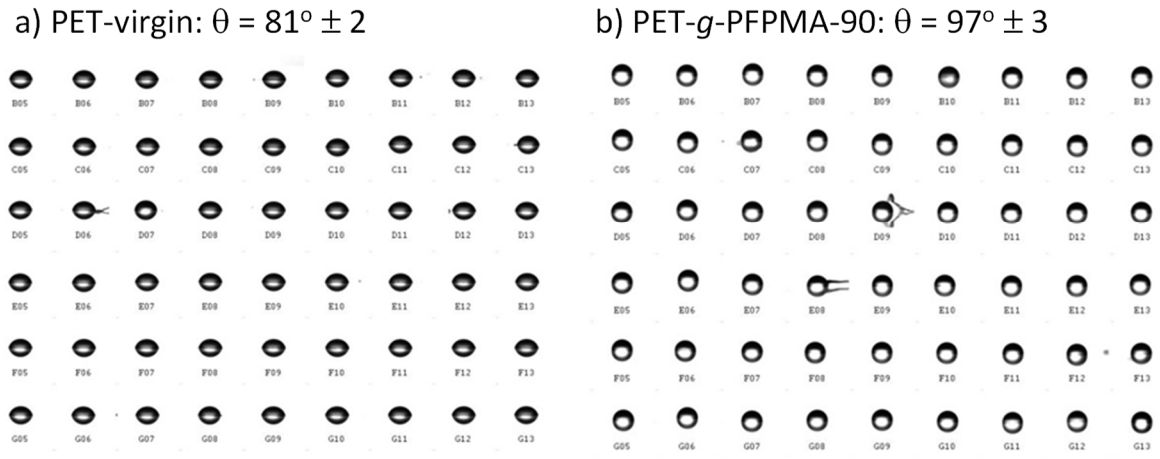

Figure 3. Images of 54 water drops deposited on the middle region of a) PET-virgin and b) PET-*g*-PFPMA-90. Full spectra of both films are presented in Figure S2 (Supporting Information).

4.3. Verification of chemical environment by ATR FTIR

ATR FTIR was employed to verify the chemical change on surface after each modification. Unfortunately, the modification of PET surface after aminolysis and immobilisation of initiator could not be confirmed by this technique, which might be attributed to the very thin layer of deposited PEI and the monolayer of initiator. In contrast, the graft of PFPMA from PET supporting surface resulted

267 in a huge obvious change in ATR FTIR spectrum (Figure 4) shown by the distinguished appearance of
268 the peak at 995 cm^{-1}, correlates to the C-F bond. Furthermore, the high conjugation within its
269 molecular structure was observed with peaks corresponding to C-O, C=C and C=O of PFPMA shifted
270 to higher wavenumbers (at 1056 cm^{-1}, 1521 cm^{-1} and 1776 cm^{-1}, respectively) compared to that
271 originated from PET and were close to those reported previously [37, 62]. It is seen that the induction in
272 hydrophobicity is associated with the increase in intensity of PFPMA recorded by FTIR. While at
273 lower contact angle, the intensity from PET is more intense than that of active polymers, FTIR
274 spectrum shows the dominance in signals originated from PFPMA at contact angle of 127° suggesting
275 that within the penetration depth of infrared light, which ranges between several hundred nanometres,
276 the quantity of active polymer is much greater than that of supporting surface.

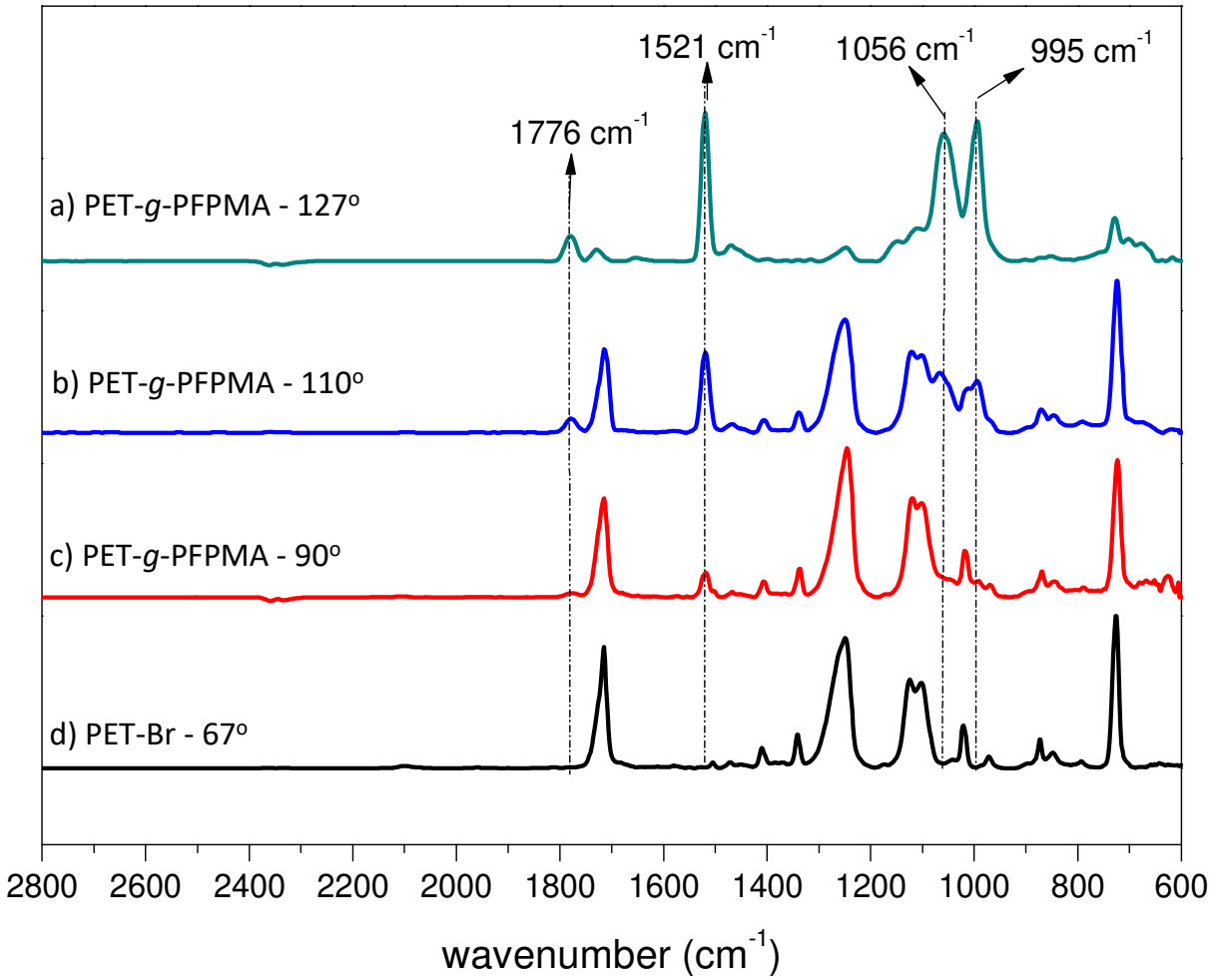

277

278 **Figure 4. ATR FTIR spectra of PET grafted with polymer of PFPMA at different**
279 **polymerisation conditions: a) 3-day small batch surface initiated Cu(0)-polymerisation, b) 1-day**

small batch surface initiated Cu(0)-polymerisation, c) 1-day large batch surface initiated Cu(0)-mediated polymerisation compared to d) PET film grafted with initiator (PET-Br). Peaks characterised for PFPMA include C=O: 1776 cm^{-1}, C=C: 1521 cm^{-1}, C-O: 1056 cm^{-1} and C-F: 995 cm^{-1}.

4.4. Chemical composition of modified surface measured by XPS

XPS analysis was carried out in order to investigate the surface chemical composition after each step modification. XPS survey of virgin PET, PET-NH_2, PET-Br, PET-*g*-PFPMA are shown in Figure 5, atomic percentages of atoms present on surfaces are summarised in Table 1 and fitting parameters as well as peak assignments are presented in Table 2.

XPS survey spectrum of virgin PET surface presents basic peaks of C1s (284 eV) and O1s (531 eV), while after PEI aminolysis, obtained surface showed the signal of N1s at 399 eV with atomic percentage contribution of 7% (Table 1, entry 2). The success of aminolysis of PET surface PEI is also confirmed by the appearance of a new contribution which corresponds to an amide N-C=O bond at 287.9 eV in C1s core level and at 530.7 eV in O1s core level of PET-NH_2 film, indicating the strong covalent attachment of the PEI to the support. Fitting results of core level of N1s region of PET-NH_2 surface (Figure 6a) indicates the dominance of C-N bonds, corresponding to 69% of total recorded signals, while the charge built up from amines takes 31 %.

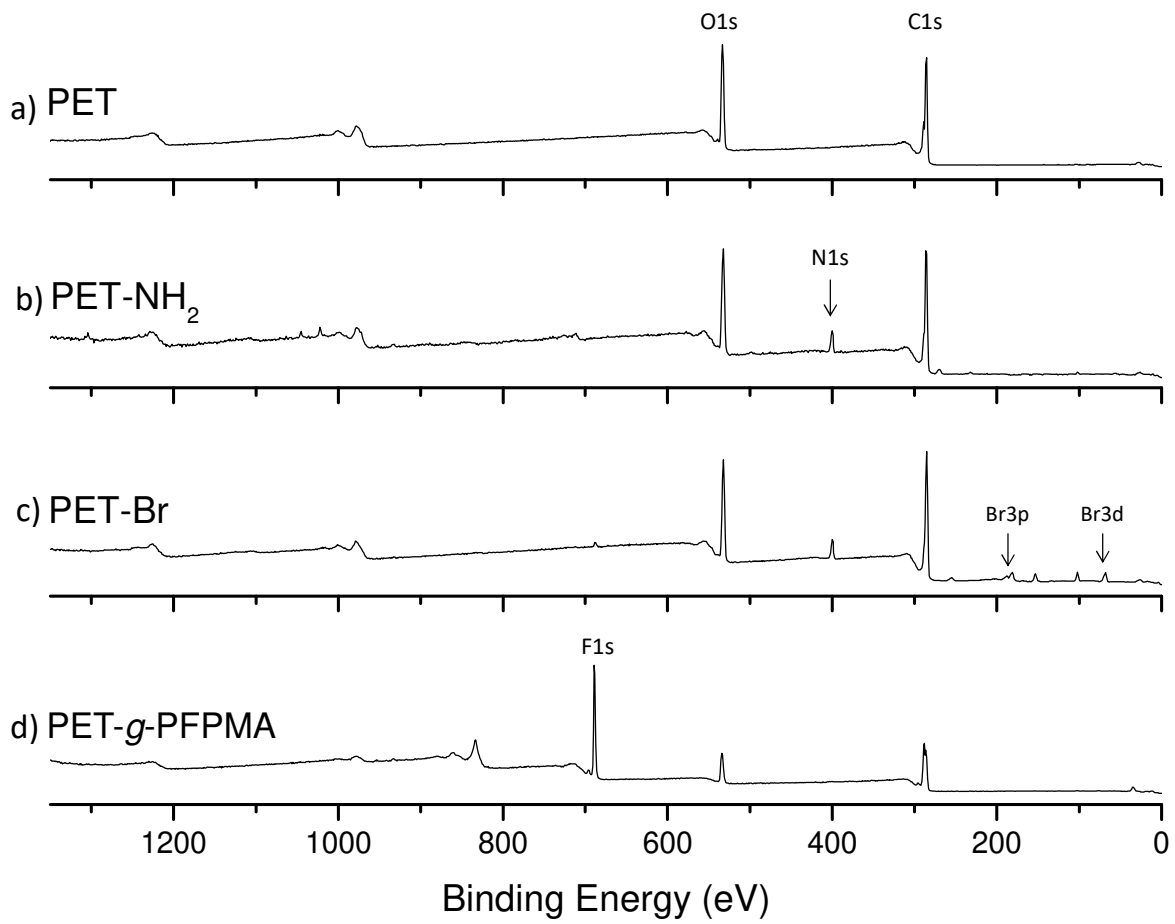

297

298 **Figure 5. XPS survey spectra of: a) virgin PET, b) PET after aminolysis, c) PET after**
299 **immobilisation of initiator, d) representative PET after surface initiated Cu(0)-mediated**
300 **polymerisation of PFPMA.**

301 **Table 1. XPS results as atomic percentage of elements detected on surface after each**
302 **modification. Values were calculated as average of 3 points of measurement for each film.**

Entry	Sample type	%C1s	%O1s	%N1s	%Br3d	%F1s
1	PET-virgin	77	23	0	0	0
2	PET-NH_2	68	25	7	0	0
3	PET-Br	70	21.5	6	2.5	0
4	PET-*g*-PFPMA-90	61	12	1	0	26
5	PET-*g*-PFPMA-110	59	12	1	0	28

6	PET-*g*-PFPMA-127	60	12	0	0	28
7	PFPMA*	59	12	0	0	29

303 * calculated from structure of monomer

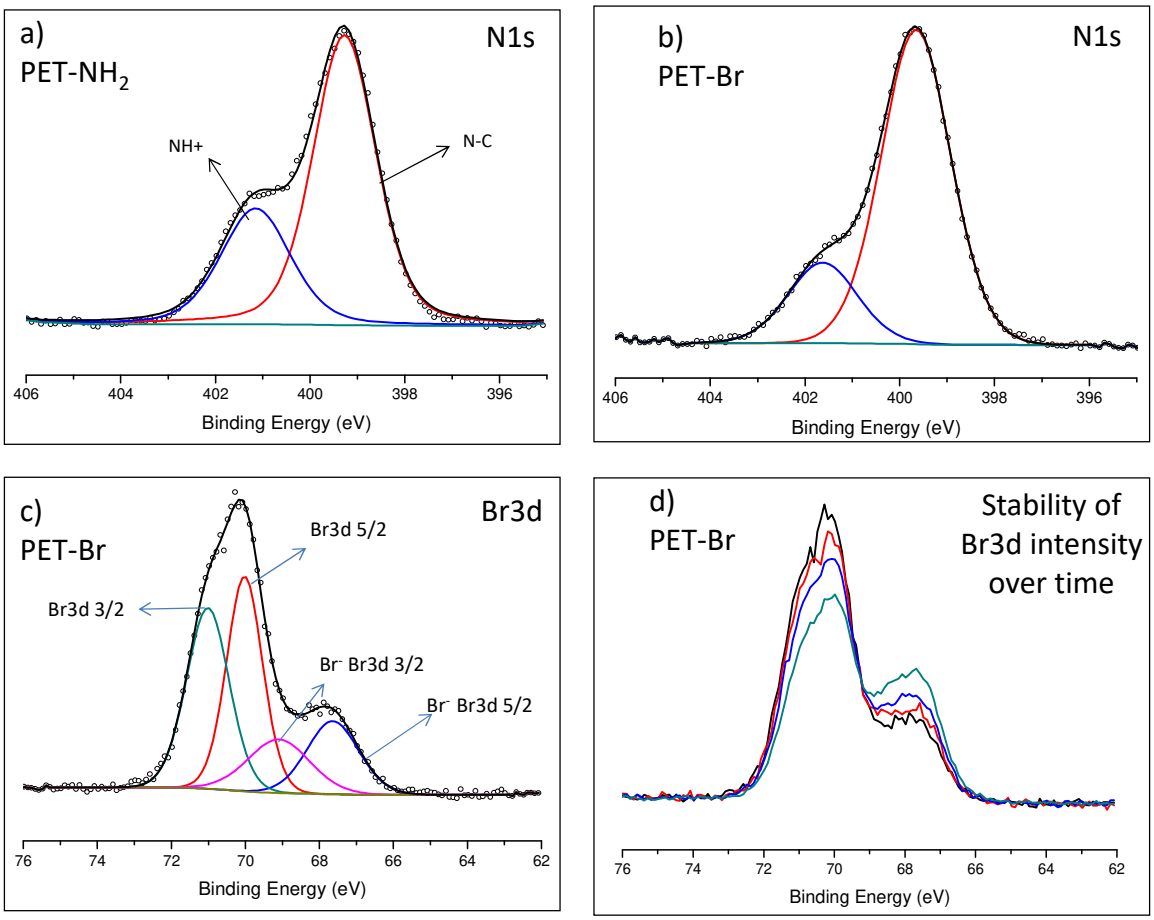

304

305 **Figure 6. Fitting results of N1s high resolution core level of a) PET-NH_2 and b) PET-Br film; c)**
306 **fitting results of Br3d core level and d) the stability of bromine species of PET-Br film.**

307 After immobilisation of initiator, the Br3d and Br3p signals appeared concomitantly with a slight
308 decrease of N1s signal intensity, confirming the initiator grafting (Figure 6c). The amount of Br3d was
309 quantified to be 2.5% in term of number atomic percentage. Nevertheless, fitting results of N1s core
310 level of PET-NH_2 (Figure 6a) and PET-Br (Figure 6b) showed a change in the ratio between C-N and
311 NH^+ due to the reaction between amines and initiator precursor. The use of PEI to graft amino groups
312 on PET surface resulted in a higher percentage of initiator on surface, proved by a higher amount of
313 Br3d recorded by XPS, which was 2.5% in this research compared to that of 1% in a previous report[25].

Figure 6c presents the fitting results of high resolution Br3d core level with 4 major contributors of neutral and charge bromine atoms. It is seen in Figure 6d that the covalently bonded initiator is stable on the surface, but a partial amount of bromine is getting charged during measurement indicated by the increase in intensity of shoulder peak at 67 eV.

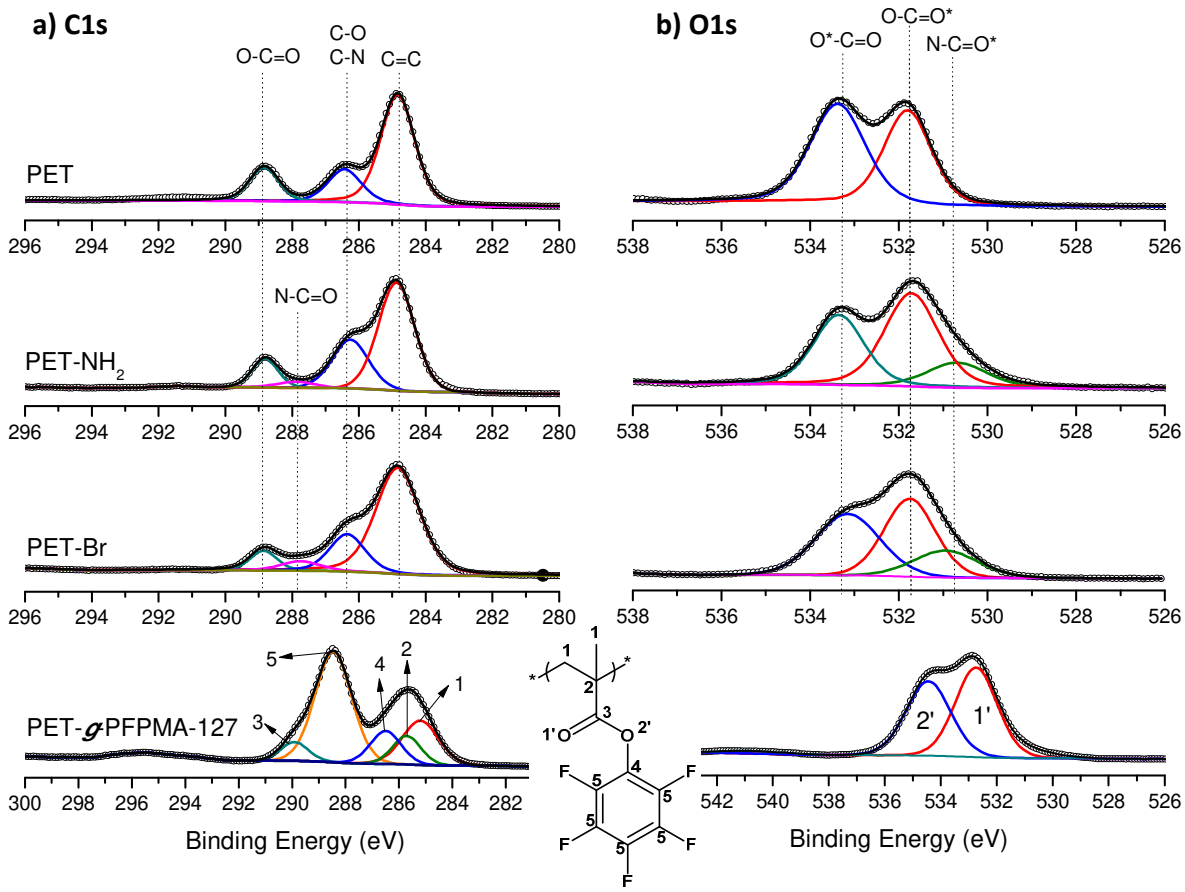

Figure 7. Fitting results of a) C1s core level scan and b) O1s core level scan of PET surface after each modification. From top to bottom: virgin PET, PET after aminolysis (PET-NH_2), PET after immobilisation of initiator (PET-Br), and PET grafted with PFPMA (PET-*g*-PFPMA)

On the other hand, the analysis of N1s and Br3d ratios with regard to C1s and O1s of PET-NH_2 and PET-Br film indicates a very thin layer of PEI and initiator grafted onto surface. This observation was in correspondence with ATR FTIR data where almost no difference among PET-virgin, PET-NH_2 and PET-Br films spectra was observed.

As the result of surface-initiated Cu(0)-mediated radical polymerisation of PFPMA from PET-Br films, an intense signal of F1s (28% in number atomic percentage) was recorded in survey scan of respective film (Figure 4. As seen from entries 4 to 7 (Table 1), albeit the water contact angle of PET-

328 *g*-PFPMA varies, all three surfaces shows close values in atomic percentage of C1s, O1s and F1s
329 compared to corresponding values calculated from the structure of the monomer. This indicates that
330 even at low contact angle (PET-*g*-PFPMA -90 films), the thickness of PFPMA grafted layer is at least
331 of the same magnitude as the penetration depth of X-ray used in this technique, i.e. around 10 nm.

332 These results in number atomic percentage confirmed that the majority of signals recorded originated
333 from grafted PFPMA moieties therefore, the negligible amount of PET signals were not considered
334 during the fitting process of PET-*g*-PFPMA surfaces.

335 **Table 2. Fitting parameters for XPS analysis of PET surface at different stages of modification.**

Core level	Bond assignment	Surface type											
		PET			PET-NH_2			PET-Br			PET-*g*-PFPMA-127		
		Peak BE	FWHM	% Area	Peak BE	FWHM	% Area	Peak BE	FWHM	% Area	Peak BE	FWHM	% Area
C1s	C-C	284.9	1.19	64.5	284.9	1.27	59.1	284.8	1.55	67.5	284.9	1.65	21.1
	C-O, C-N	286.5	1.17	18.7	286.3	1.26	26.4	286.4	1.25	19.2	286.2	1.21	10.5
	COO	288.9	1.01	16.8	288.8	0.89	10.7	288.9	0.94	7.7	289.7	1.12	5.2
	N-C=O				287.9	1.45	2.8	287.7	1.42	5.6			
	$C-CH_3$										285.4	1.65	10.5
	C-F										288.1	1.67	52.7
O1s	C=O	532.0	1.27	50	531.7	1.44	50.1	531.8	1.35	41.2	532.6	1.70	52.4
	C-O	533.6	1.46	50	533.3	1.30	35.0	533.2	1.70	40.8	534.3	1.84	47.6
	N-C=O				530.7	1.60	14.9	531.0	1.72	18.0			
N1s	N-C				399.3	1.56	69.0	399.7	1.72	79.6			
	NH^+				401.2	1.74	31.0	401.6	1.72	20.4			
Br3d	Br3d 3/2							71.0	1.35	34.1			
	Br3d 5/2							70.0	1.15	34.40			
	Br-3d 3/2							69.1	1.97	14.7			
	Br-3d 5/2							67.6	1.65	17.8			
F1s	C-F										688.2	1.74	100

336 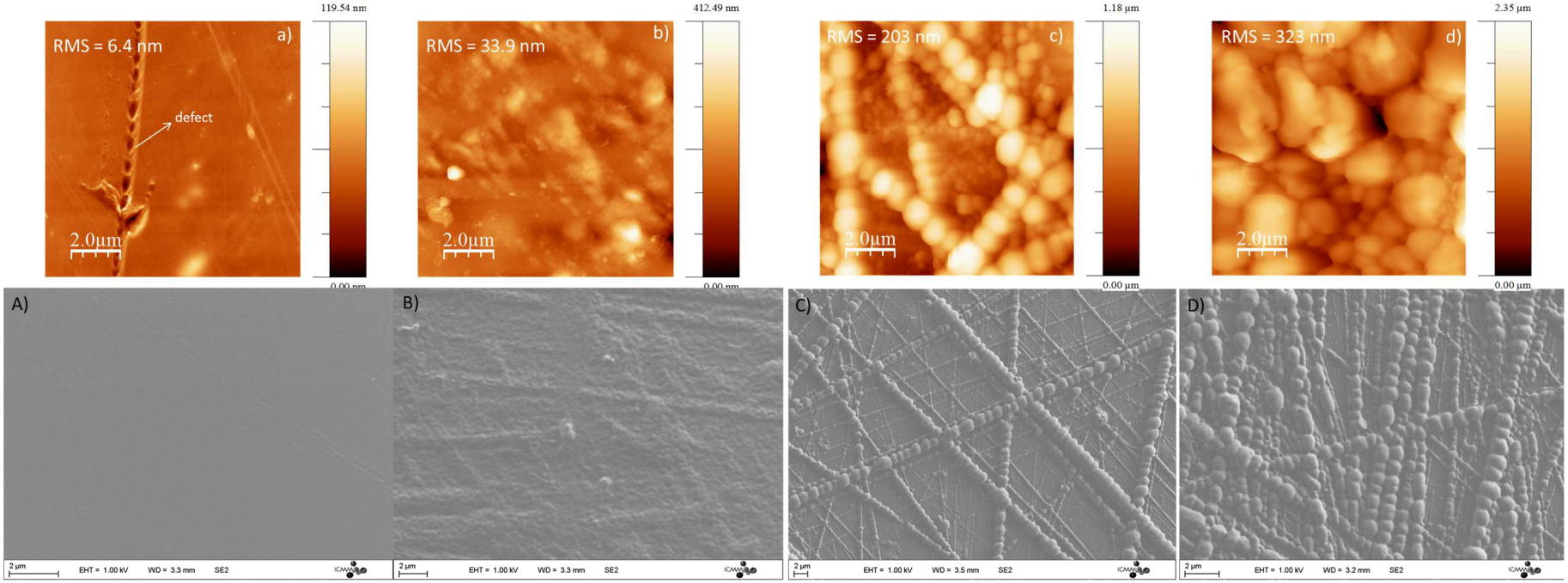

337 **Figure 8. Topology of PET surfaces grafted with initiator and PFPMA polymers at different reaction conditions observed by tapping mode AFM (on**
338 **top) and SEM (bottom), from left to right: a, A) PET-Br; b, B) PET-*g*-PFPMA-90; c, C) PET-*g*-PFPMA-110; d, D) PET-*g*-PFPMA-127. Onset RMS**
339 **indicates root-mean-square roughness of corresponding surfaces.**

340

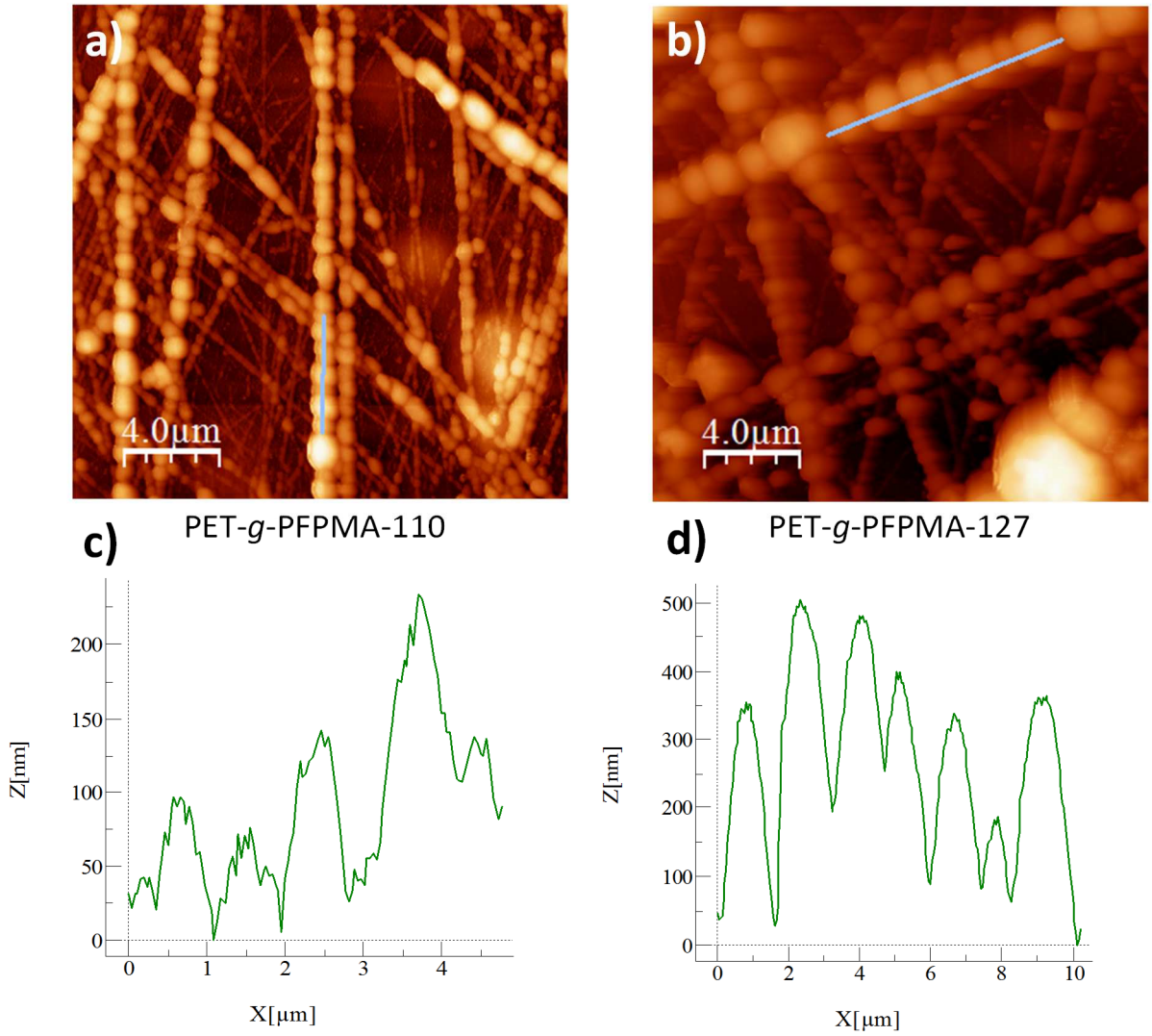

Figure 9. AFM images (top) and results of profiling a representative chain of islands on PET-*g*-PFPMA surfaces (bottom). a, c) PET-*g*-PFPMA-110 surface; b, d) PET-*g*-PFPMA-127 surface

As seen in **Figure 7**, the core level scan of C1s can be deconvoluted according to the chemical structure of PFPMA, which includes carbon atoms of: aliphatic carbons (284.9 eV), quaternary *C*-CH_3 (285.4 eV), conjugated *C*OO (289.7 eV), C=*C*-O (286.2 eV), *C*-F (288.1 eV) and π-π* shake-up (295.5 eV). These assignations present a good agreement to those reported in literature [37, 62]. O1s core level profile could be deconvoluted into 2 major contributions of C=O at 532.6 eV and C-O at 534.3 eV. These values are approximately 1eV higher compared to carbonyl oxygen of PET, this is reasonable because ATR FTIR spectra (Figure 4) of PET-*g*-PFPMA surfaces show that the carbonyl C-O and C=O of PFPMA are also shifted to higher wavenumber compared to that of PET, indicating

352 the difference in chemical environment between carbonyl groups bonds of the supporting surface and
353 the active ester polymer.

354 **4.5. Topology of PET-*g*-PFPMA films by AFM and SEM**

355 Surface topology and RMS of PET-v, PET-Br and PET-*g*-PFPMA were then observed with AFM and
356 SEM (Figure 8). The change in topology of PET films before and after surface initiated polymerisation
357 was remarkable. PET-Br surface appeared to be smooth as observed in SEM image (Figure 8A);
358 besides, AFM (Figure 8a) showed a RMS value of 6.4 nm. The surface roughness increased visually
359 after polymerisation. As seen by both AFM and SEM (Figure 8b and Figure 8B), the change in
360 topology of the PET-*g*-PFPMA-90 films was obvious compared to that of PET-Br films, which caused
361 a surface of higher roughness (RMS of 6.4 nm and 33.9 nm before and after polymerisation,
362 respectively). With regard to surface topology, while AFM exhibited the appearance of islands on the
363 surface, SEM provided a wider image, which showed that there was a structural development. The
364 change in topology was more pronounced in the case of PET-*g*-PFPMA-110 and PET-*g*-PFPMA-127
365 with RMS increased to 203 nm and 323 nm, respectively. On these surfaces, well-oriented chains of
366 islands were also recognized from both AFM and SEM images. Profiling these chains (Figure 9)
367 indicated that, on the same film, each island along the chain was of approximately the same size to
368 another; however, there was an increase in size when the polymerisation time was prolonged. PET-*g*-
369 PFPMA-110 had islands of around 1 micron in width whereas for PET-*g*-PFPMA-127 surface, the
370 island's size was approximately 1.8 micron in width. On the other hand, as seen by XPS, the extreme
371 surfaces of all three types of PET-*g*-PFPMA had the same chemical composition, yet the wettability of
372 the three surfaces varied. This phenomenon could be explained by the increase in surface roughness,
373 which reinforces the hydrophobicity or hydrophilicity of a surface[63]. It is necessary to note that after
374 24 hours of Soxhlet extraction in THF, the same contact angle and identical AFM images were
375 recorded, indicating the strong attachment of the polymer of PFPMA onto PET surface.

376 **4.6. Post-modification of PET-G-PFPMA-90 films with geraniol**

377 To confirm the reactivity of grafted PFPMA polymer, PET-*g*-PFPMA-90 films were post-modified
378 with geraniol via transesterification in DMF at 50°C in presence of DBU to obtain PET grafted with
379 polymer of geranyl methacrylate (PET-*g*-GeMA) (Figure 10). The first indicator of the success in
380 post-modification was the significant drop in water contact angle (from 90° to 74°) due to the
381 replacement of pentafluorophenyl moieties by the less hydrophobic geranyl groups. The substitution
382 was further confirmed by ATR FTIR with the disappearance of peaks corresponding to C=O (1776
383 cm^{-1}), C=C (1521 cm^{-1}) and C-F (995 cm^{-1}) (Figure 11b,c) of PFPMA.

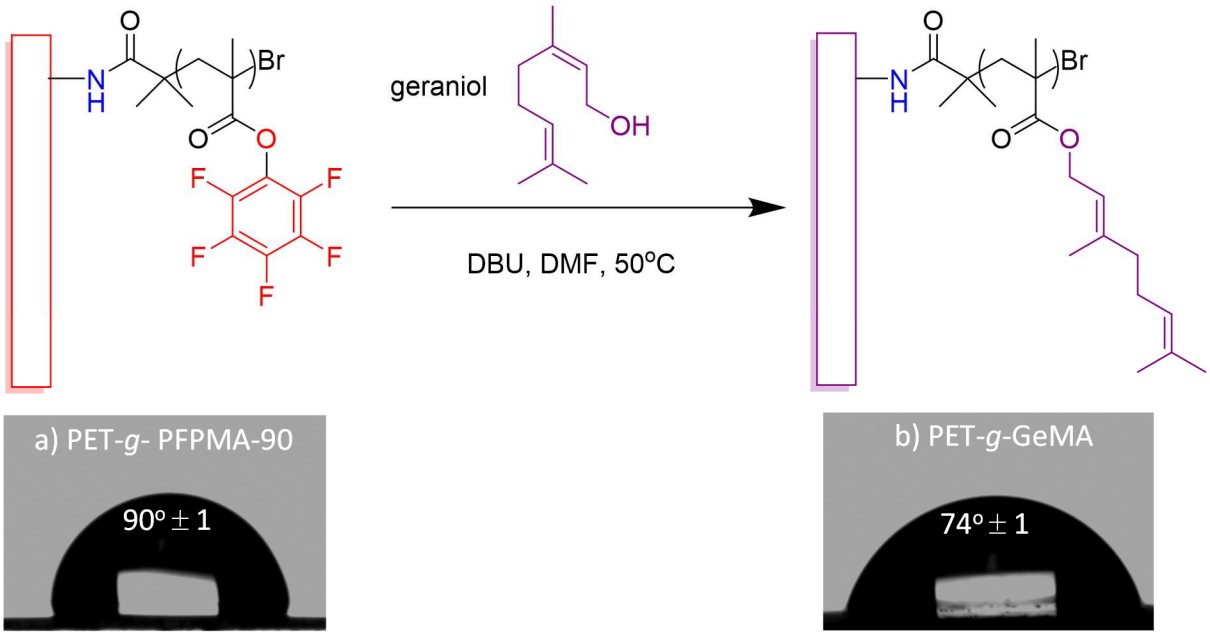

384

385 **Figure 10. Transesterification of PET-*g*-PFPMA-90 films with geraniol and water contact angle**
386 **of films obtained before (a) and after (b) post-modification.**

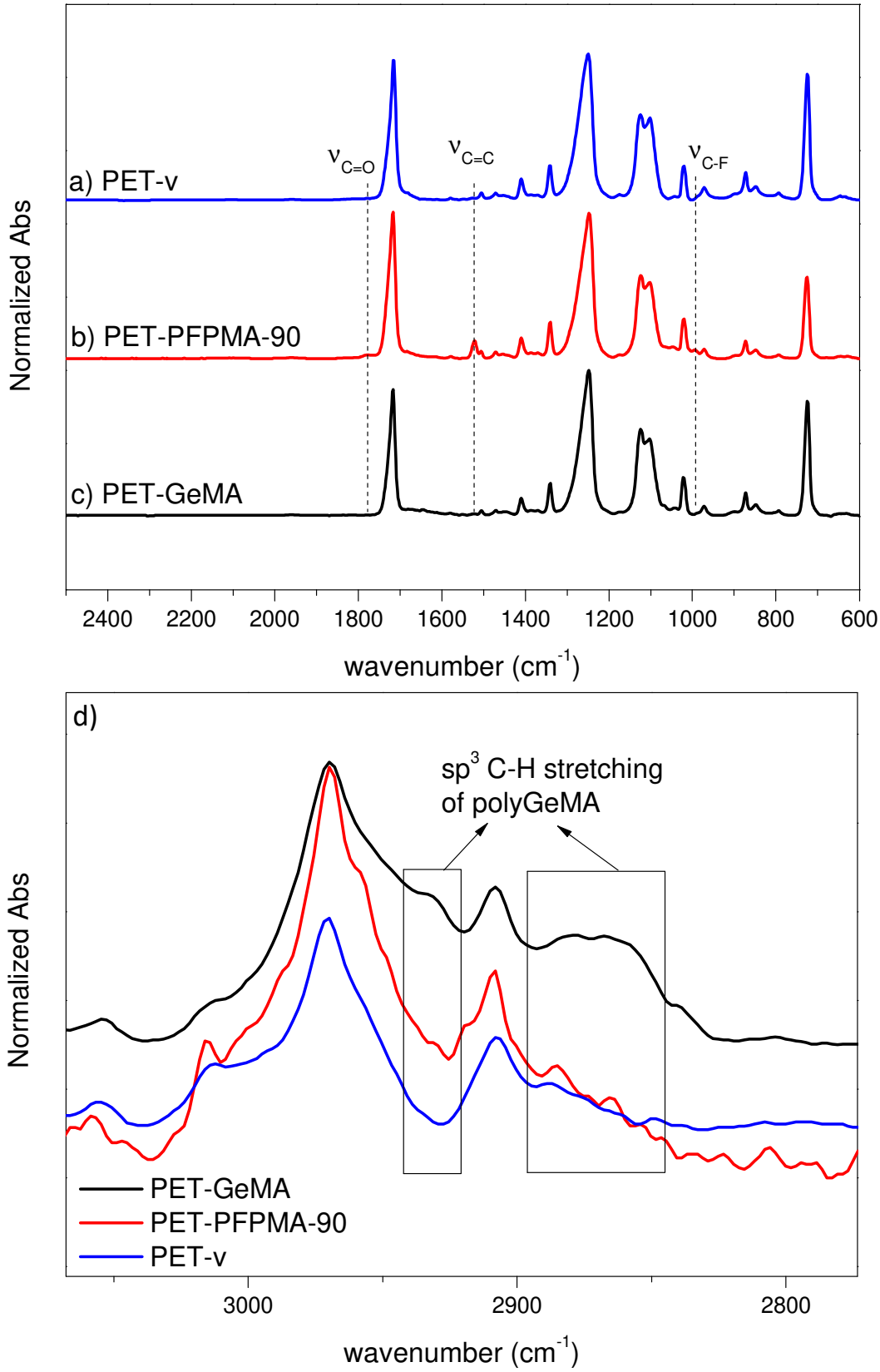

387

388 **Figure 11. ATR FTIR spectra of PET-virgin (a), PET-*g*-PFPMA-90 before modification (b),**

389 **PET-GeMA obtained after post-modification, and a comparison in C-H stretching region (d).**

Unfortunately, the peaks originated from polymer of geranyl methacrylate (Figure 10c) could not be distinguished clearly from that of PET support (Figure 10a) due to similarity in their chemical environment. The only pronounced difference is the appearance of peaks characterized to the sp^3 C-H stretching of geranyl group at 2931 cm^{-1} and a broad peak from 2844-2892 cm^{-1} (Figure 11d).

5. Conclusion

A sequential chemical modification process of PET surface has been proposed and proved to be effective. The process includes aminolysis of PET virgin surface, followed by the immobilisation of initiator and finally the surface-initiated Cu(0)-mediated polymerisation of PFPMA. Each modification step was evaluated qualitatively and quantitatively by several analysis methods including water contact angle, titration with orange II dye, ATR FTIR and XPS. By varying polymerisation conditions and scales, PET-*g*-PFPMA surfaces showed the change in surface roughness and topology as observed by AFM and SEM, which, in consequence, led to the change of surface wettability. Therefore, surface-initiated Cu(0)-mediated radical polymerisation has been shown to be a good alternative for easy grafting of PFPMA polymer from PET surface. Furthermore, with the ease in post-modification of PFPMA polymer proved by the transesterification with geraniol, this approach opens the possibility to introduce onto PET surface a wide variety of other functional groups with borderless applications.

Confliction

Authors of this research declare to possess no interest confliction.

Acknowledgments

Authors of this research would like to acknowledge the Centre National de la Recherche Scientifique (CNRS) and the Ministère de l'Enseignement supérieur, de la Recherche et de l'Innovation (M.E.S.R.I.) of France for their financial support on the project. We would like to thank Tom Metayer and Daphné Hector for the experimental contributions at the beginning of the work.

References

1. Zhu, Y.; Gao, C.; Liu, X.; Shen, J., Surface modification of polycaprolactone membrane via aminolysis and biomacromolecule immobilization for promoting cytocompatibility of human endothelial cells. *Biomacromolecules* **2002,** *3* (6), 1312-1319.

2. Goddard, J. M.; Hotchkiss, J. H., Polymer surface modification for the attachment of bioactive compounds. *Progress in Polymer Science* **2007,** *32* (7), 698-725.

3. Yang, X.; Zhao, K.; Chen, G.-Q., Effect of surface treatment on the biocompatibility of microbial polyhydroxyalkanoates. *Biomaterials* **2002,** *23* (5), 1391-1397.

4. Kim, J. A.; Seong, D. G.; Kang, T. J.; Youn, J. R., Effects of surface modification on rheological and mechanical properties of CNT/epoxy composites. *Carbon* **2006,** *44* (10), 1898-1905.

5. Eitan, A.; Jiang, K.; Dukes, D.; Andrews, R.; Schadler, L. S., Surface modification of multiwalled carbon nanotubes: toward the tailoring of the interface in polymer composites. *Chemistry of Materials* **2003,** *15* (16), 3198-3201.

6. Kim, S. W.; Kim, T.; Kim, Y. S.; Choi, H. S.; Lim, H. J.; Yang, S. J.; Park, C. R., Surface modifications for the effective dispersion of carbon nanotubes in solvents and polymers. *Carbon* **2012,** *50* (1), 3-33.

7. Ma, Z.; Mao, Z.; Gao, C., Surface modification and property analysis of biomedical polymers used for tissue engineering. *Colloids and Surfaces B: Biointerfaces* **2007,** *60* (2), 137-157.

8. Chen, N.; Kim, D. H.; Kovacik, P.; Sojoudi, H.; Wang, M.; Gleason, K. K., Polymer thin films and surface modification by chemical vapor deposition: Recent progress. *Annual review of chemical and biomolecular engineering* **2016,** *7*, 373-393.

9. Sheng, W.; Li, B.; Wang, X.; Dai, B.; Yu, B.; Jia, X.; Zhou, F., Brushing up from "anywhere" under sunlight: a universal surface-initiated polymerization from polydopamine-coated surfaces. *Chemical science* **2015,** *6* (3), 2068-2073.

10. Guo, S.; Jańczewski, D.; Zhu, X.; Quintana, R.; He, T.; Neoh, K. G., Surface charge control for zwitterionic polymer brushes: Tailoring surface properties to antifouling applications. *Journal of colloid and interface science* **2015,** *452*, 43-53.

11. Guo, H. C.; Ye, E.; Li, Z.; Han, M.-Y.; Loh, X. J., Recent progress of atomic layer deposition on polymeric materials. *Materials Science and Engineering: C* **2017,** *70*, 1182-1191.

12. Awaja, F.; Pavel, D., Recycling of PET. *European Polymer Journal* **2005,** *41* (7), 1453-1477.

13. Sinha, V.; Patel, M. R.; Patel, J. V., PET waste management by chemical recycling: a review. *Journal of Polymers and the Environment* **2010,** *18* (1), 8-25.

14. Boulares-Pender, A.; Prager, A.; Reichelt, S.; Elsner, C.; Buchmeiser, M. R., Functionalization of plasma-treated polymer surfaces with glycidol. *Journal of Applied Polymer Science* **2011,** *121* (5), 2543-2550.

15. Ramires, P. A.; Mirenghi, L.; Romano, A. R.; Palumbo, F.; Nicolardi, G., Plasma-treated PET surfaces improve the biocompatibility of human endothelial cells. *Journal of Biomedical Materials Research* **2000,** *51* (3), 535-539.

16. Sun, J.; Yao, L.; Gao, Z.; Peng, S.; Wang, C.; Qiu, Y., Surface modification of PET films by atmospheric pressure plasma-induced acrylic acid inverse emulsion graft polymerization. *Surface and Coatings Technology* **2010,** *204* (24), 4101-4106.

17. Utrata-Wesołek, A.; Wałach, W.; Bochenek, M.; Trzebicka, B.; Anioł, J.; Sieroń, A. L.; Kubacki, J.; Dworak, A., Branched polyglycidol and its derivatives grafted-from poly(ethylene terephthalate) and silica as surfaces that reduce protein fouling. *European Polymer Journal* **2018,** *105*, 313-322.

18. Zhang, Z. Y.; Boyd, I. W.; Esrom, H., Surface Modification of Polyethylene Terephthalate with Excimer UV Radiation. *Surface and Interface Analysis* **1996,** *24* (10), 718-722.

19. Gao, S. L.; Häßler, R.; Mäder, E.; Bahners, T.; Opwis, K.; Schollmeyer, E., Photochemical surface modification of PET by excimer UV lamp irradiation. *Applied Physics B* **2005,** *81* (5), 681-690.

20. Salmi-Mani, H.; Terreros, G.; Barroca-Aubry, N.; Aymes-Chodur, C.; Regeard, C.; Roger, P., Poly(ethylene terephthalate) films modified by UV-induced surface graft polymerization of vanillin derived monomer for antibacterial activity. *European Polymer Journal* **2018,** *103*, 51-58.

21. Fávaro, S.; Rubira, A.; Muniz, E.; Radovanovic, E., Surface modification of HDPE, PP, and PET films with KMnO4/HCl solutions. *Polymer Degradation and Stability* **2007,** *92* (7), 1219-1226.

22. Loïc, B.; Thierry, M.; Bénédicte, L.; Philippe, R., Chemical surface modification of poly(ethylene terephthalate) fibers by aminolysis and grafting of carbohydrates. *Journal of Polymer Science Part A: Polymer Chemistry* **2007,** *45* (11), 2172-2183.

23. Golshaei, P.; Güven, O., Chemical modification of PET surface and subsequent graft copolymerization with poly (N-isopropylacrylamide). *Reactive and Functional Polymers* **2017,** *118*, 26-34.

24. Lepoittevin, B.; Costa, L.; Pardoue, S.; Dragoé, D.; Mazerat, S.; Roger, P., Hydrophilic PET surfaces by aminolysis and glycopolymer brushes chemistry. *Journal of Polymer Science Part A: Polymer Chemistry* **2016,** *54* (17), 2689-2697.

25. Bedel, S.; Lepoittevin, B.; Costa, L.; Leroy, O.; Dragoe, D.; Bruzaud, J.; Herry, J.-M.; Guilbaud, M.; Bellon-Fontaine, M.-N.; Roger, P., Antibacterial poly(ethylene terephthalate) surfaces obtained from thymyl methacrylate polymerization. *Journal of Polymer Science Part A: Polymer Chemistry* **2015,** *53* (17), 1975-1985.

26. Lepoittevin, B.; Bedel, S.; Dragoé, D.; Bruzaud, J.; Barthés-Labrousse, M.-G.; Mazerat, S.; Herry, J.-M.; Bellon-Fontaine, M.-N.; Roger, P., Antibacterial surfaces obtained through dopamine and fluorination functionalizations. *Progress in Organic Coatings* **2015,** *82*, 17-25.

27. Ou, J.; Wang, J.; Zhang, D.; Zhang, P.; Liu, S.; Yan, P.; Liu, B.; Yang, S., Fabrication and biocompatibility investigation of TiO2 films on the polymer substrates obtained via a novel and versatile route. *Colloids and Surfaces B: Biointerfaces* **2010,** *76* (1), 123-127.

28. Cai, X.; Yuan, J.; Chen, S.; Li, P.; Li, L.; Shen, J., Hemocompatibility improvement of poly(ethylene terephthalate) via self-polymerization of dopamine and covalent graft of zwitterions. *Materials Science and Engineering: C* **2014,** *36*, 42-48.

29. Pan, K.; Ren, R.; Li, H.; Cao, B., Preparation of dual stimuli-responsive PET track-etched membrane by grafting copolymer using ATRP. *Polymers for Advanced Technologies* **2013,** *24* (1), 22-27.

30. Maaz, M.; Elzein, T.; Bejjani, A.; Barroca-Aubry, N.; Lepoittevin, B.; Dragoe, D.; Mazerat, S.; Nsouli, B.; Roger, P., Surface initiated supplemental activator and reducing agent atom transfer radical polymerization (SI-SARA-ATRP) of 4-vinylpyridine on poly(ethylene terephthalate). *Journal of Colloid and Interface Science* **2017,** *500*, 69-78.

31. Das, A.; Theato, P., Activated Ester Containing Polymers: Opportunities and Challenges for the Design of Functional Macromolecules. *Chemical Reviews* **2016,** *116* (3), 1434-1495.

32. Theato, P., Synthesis of well-defined polymeric activated esters. *Journal of Polymer Science Part A: Polymer Chemistry* **2008,** *46* (20), 6677-6687.

33. Hwang, J.; Li, R. C.; Maynard, H. D., Well-defined polymers with activated ester and protected aldehyde side chains for bio-functionalization. *Journal of Controlled Release* **2007,** *122* (3), 279-286.

34. Eberhardt, M.; Mruk, R.; Zentel, R.; Théato, P., Synthesis of pentafluorophenyl(meth)acrylate polymers: New precursor polymers for the synthesis of multifunctional materials. *European Polymer Journal* **2005,** *41* (7), 1569-1575.

35. Noy, J.-M.; Koldevitz, M.; Roth, P. J., Thiol-reactive functional poly (meth) acrylates: multicomponent monomer synthesis, RAFT (co) polymerization and highly efficient thiol–para-fluoro postpolymerization modification. *Polymer Chemistry* **2015,** *6* (3), 436-447.

36. Delaittre, G.; Barner, L., The para-fluoro-thiol reaction as an efficient tool in polymer chemistry. *Polymer Chemistry* **2018,** *9* (20), 2679-2684.

37. Gunay, K. A.; Schuwer, N.; Klok, H.-A., Synthesis and post-polymerization modification of poly(pentafluorophenyl methacrylate) brushes. *Polymer Chemistry* **2012,** *3* (8), 2186-2192.

38. Wilaiporn, G.; Hui, Z.; Suda, K.; Patrick, T.; P., H. V., Formation of thermo-sensitive and cross-linkable micelles by self-assembly of poly(pentafluorophenyl acrylate)-containing block copolymer. *Journal of Polymer Science Part A: Polymer Chemistry* **2015,** *53* (9), 1103-1113.

39. Eberhardt, M.; Théato, P., RAFT polymerization of pentafluorophenyl methacrylate: preparation of reactive linear diblock copolymers. *Macromolecular rapid communications* **2005,** *26* (18), 1488-1493.

40. Lee, Y.; Hanif, S.; Theato, P.; Zentel, R.; Lim, J.; Char, K., Facile Synthesis of Fluorescent Polymer Nanoparticles by Covalent Modification–Nanoprecipitation of Amine-Reactive Ester Polymers. *Macromolecular Rapid Communications* **2015,** *36* (11), 1089-1095.

41. Singha, N. K.; Gibson, M. I.; Koiry, B. P.; Danial, M.; Klok, H.-A., Side-Chain Peptide-Synthetic Polymer Conjugates via Tandem "Ester-Amide/Thiol–Ene" Post-Polymerization Modification of Poly(pentafluorophenyl methacrylate) Obtained Using ATRP. *Biomacromolecules* **2011,** *12* (8), 2908-2913.

42. Khan, M.; Yang, J.; Shi, C.; Lv, J.; Feng, Y.; Zhang, W., Surface tailoring for selective endothelialization and platelet inhibition via a combination of SI-ATRP and click chemistry using Cys–Ala–Gly-peptide. *Acta Biomaterialia* **2015,** *20*, 69-81.

43. Huang, Z.; Feng, C.; Guo, H.; Huang, X., Direct functionalization of poly(vinyl chloride) by photo-mediated ATRP without a deoxygenation procedure. *Polymer Chemistry* **2016,** *7* (17), 3034-3045.

44. Xu, L. Q.; Neoh, K.-G.; Kang, E.-T.; Fu, G. D., Rhodamine derivative-modified filter papers for colorimetric and fluorescent detection of Hg2+ in aqueous media. *Journal of Materials Chemistry A* **2013,** *1* (7), 2526-2532.

45. Matyjaszewski, K.; Coca, S.; Gaynor, S. G.; Wei, M.; Woodworth, B. E., Zerovalent metals in controlled/"living" radical polymerization. *Macromolecules* **1997,** *30* (23), 7348-7350.

46. Zou, Y.; Kizhakkedathu, J. N.; Brooks, D. E., Surface Modification of Polyvinyl Chloride Sheets via Growth of Hydrophilic Polymer Brushes. *Macromolecules* **2009,** *42* (9), 3258-3268.

47. Ding, S.; Floyd, J. A.; Walters, K. B., Comparison of surface confined ATRP and SET-LRP syntheses for a series of amino (meth)acrylate polymer brushes on silicon substrates. *Journal of Polymer Science Part A: Polymer Chemistry* **2009,** *47* (23), 6552-6560.

48. Lee, S. H.; Dreyer, D. R.; An, J.; Velamakanni, A.; Piner, R. D.; Park, S.; Zhu, Y.; Kim, S. O.; Bielawski, C. W.; Ruoff, R. S., Polymer Brushes via Controlled, Surface-Initiated Atom Transfer Radical Polymerization (ATRP) from Graphene Oxide. *Macromolecular Rapid Communications* **2010,** *31* (3), 281-288.

49. Thomson, D. A. C.; Cooper, M. A., A paramagnetic-reporter two-particle system for amplification-free detection of DNA in serum. *Biosensors and Bioelectronics* **2013,** *50*, 499-501.

50. Thomson, D. A. C.; Tee, E. H. L.; Tran, N. T. D.; Monteiro, M. J.; Cooper, M. A., Oligonucleotide and Polymer Functionalized Nanoparticles for Amplification-Free Detection of DNA. *Biomacromolecules* **2012,** *13* (6), 1981-1989.

51. Chen, X.; Yuan, L.; Yang, P.; Hu, J.; Yang, D., Covalent polymeric modification of graphene nanosheets via surface-initiated single-electron-transfer living radical polymerization. *Journal of Polymer Science Part A: Polymer Chemistry* **2011,** *49* (23), 4977-4986.

52. Liu, Z.; Zhu, S.; Li, Y.; Li, Y.; Shi, P.; Huang, Z.; Huang, X., Preparation of graphene/poly(2-hydroxyethyl acrylate) nanohybrid materials via an ambient temperature "grafting-from" strategy. *Polymer Chemistry* **2015,** *6* (2), 311-321.

53. Xue, L.; Lyu, Z.; Shi, X.; Tang, Z.; Chen, G.; Chen, H., Fast and Green Synthesis of a Smart Glyco-surface via Aqueous Single Electron Transfer-Living Radical Polymerization. *Macromolecular Chemistry and Physics* **2014,** *215* (15), 1491-1497.

54. Chabrol, V.; Léonard, D.; Zorn, M.; Reck, B.; D'Agosto, F.; Charleux, B., Efficient Copper-Mediated Surface-Initiated Polymerization from Raw Polymer Latex in Water. *Macromolecules* **2012,** *45* (7), 2972-2980.

55. Horcas, I.; Fernández, R.; Gómez-Rodríguez, J. M.; Colchero, J.; Gómez-Herrero, J.; Baro, A. M., WSXM: A software for scanning probe microscopy and a tool for nanotechnology. *Review of Scientific Instruments* **2007,** *78* (1), 013705.

56. Noel, S.; Liberelle, B.; Robitaille, L.; De Crescenzo, G., Quantification of Primary Amine Groups Available for Subsequent Biofunctionalization of Polymer Surfaces. *Bioconjugate Chemistry* **2011,** *22* (8), 1690-1699.

57. Chen, W.; McCarthy, T. J., Chemical Surface Modification of Poly(ethylene terephthalate). *Macromolecules* **1998,** *31* (11), 3648-3655.

58. Liu, Y.; He, T.; Gao, C., Surface modification of poly(ethylene terephthalate) via hydrolysis and layer-by-layer assembly of chitosan and chondroitin sulfate to construct cytocompatible layer for human endothelial cells. *Colloids and Surfaces B: Biointerfaces* **2005,** *46* (2), 117-126.

59. Bech, L.; Elzein, T.; Meylheuc, T.; Ponche, A.; Brogly, M.; Lepoittevin, B.; Roger, P., Atom transfer radical polymerization of styrene from different poly(ethylene terephthalate) surfaces: Films, fibers and fabrics. *European Polymer Journal* **2009,** *45* (1), 246-255.

60. Yamamoto, S.; Ejaz, M.; Tsujii, Y.; Matsumoto, M.; Fukuda, T., Surface Interaction Forces of Well-Defined, High-Density Polymer Brushes Studied by Atomic Force Microscopy. 1. Effect of Chain Length. *Macromolecules* **2000,** *33* (15), 5602-5607.

61. Wu, T.; Efimenko, K.; Genzer, J., Combinatorial Study of the Mushroom-to-Brush Crossover in Surface Anchored Polyacrylamide. *Journal of the American Chemical Society* **2002,** *124* (32), 9394-9395.

62. Francesch, L.; Borros, S.; Knoll, W.; Förch, R., Surface Reactivity of Pulsed-Plasma Polymerized Pentafluorophenyl Methacrylate (PFM) toward Amines and Proteins in Solution. *Langmuir* **2007,** *23* (7), 3927-3931.

63. Quéré, D., Rough ideas on wetting. *Physica A: Statistical Mechanics and its Applications* **2002,** *313* (1), 32-46.

591 # Supporting Information

592 # Facile and efficient Cu(0)-mediated radical polymerization
593 # of pentafluorophenyl methacrylate grafting from
594 # poly(ethylene terephthalate) (PET) film

595 *Thi Phuong Thu Nguyen [a], Nadine Barroca-Aubry [a], Diana Dragoe [a], Sandra Mazerat [a], François*
596 *Brisset[a], Jean-Marie Herry[b], Philippe Roger[a] **

597 [a] Institut de Chimie Moléculaire et des Matériaux d'Orsay (ICMMO), UMR 8182, Univ. Paris Sud,
598 Université Paris Saclay, 91405, Orsay, France

599 [b] INRA, AgroParisTech, Université Paris Saclay, UMR 782, GMPA, Ecomic, 1, avenue des
600 Olympiades, Massy F-91300, France

601 *Corresponding Author: *philippe.roger@u-psud.fr*

602

603 **Large batch polymerization tools and setup**

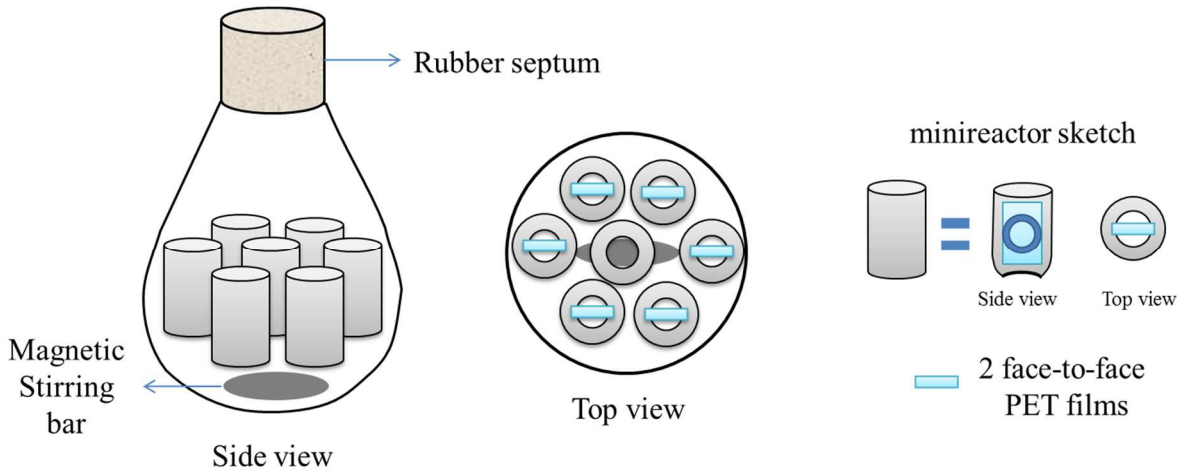

604

605

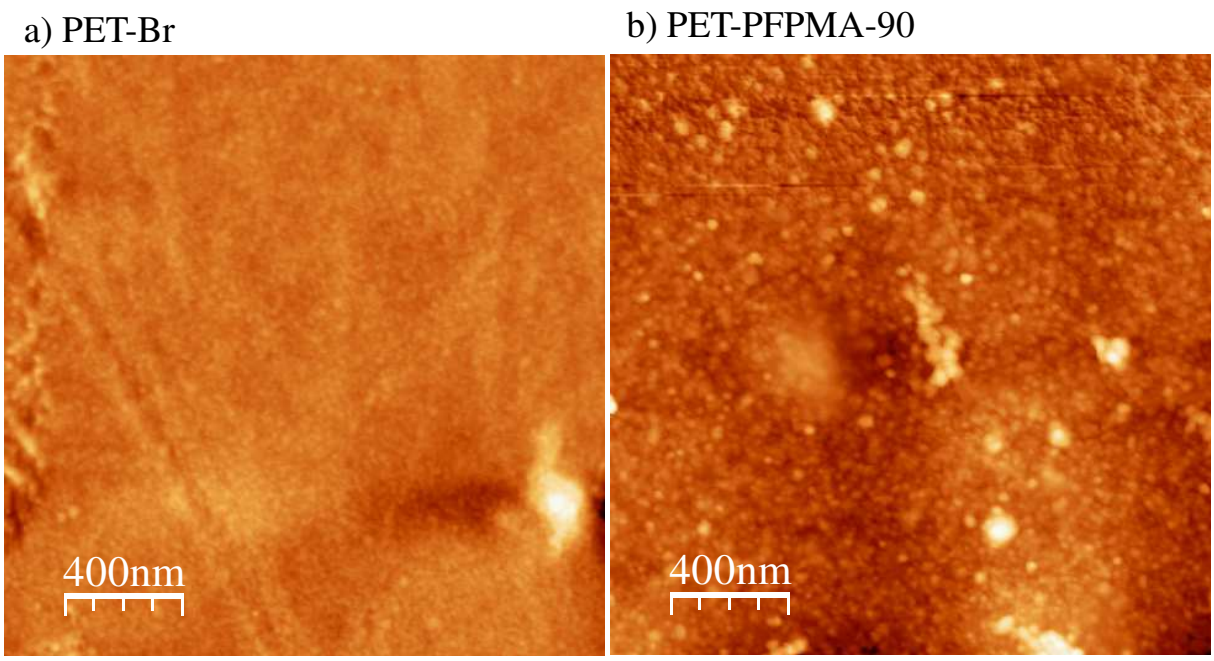

606 **Figure S 1. AFM images of a) PET-Br and b) PET-g-PFPMA-90 at 2μm x 2μm window.**

607

a) PET-virgin

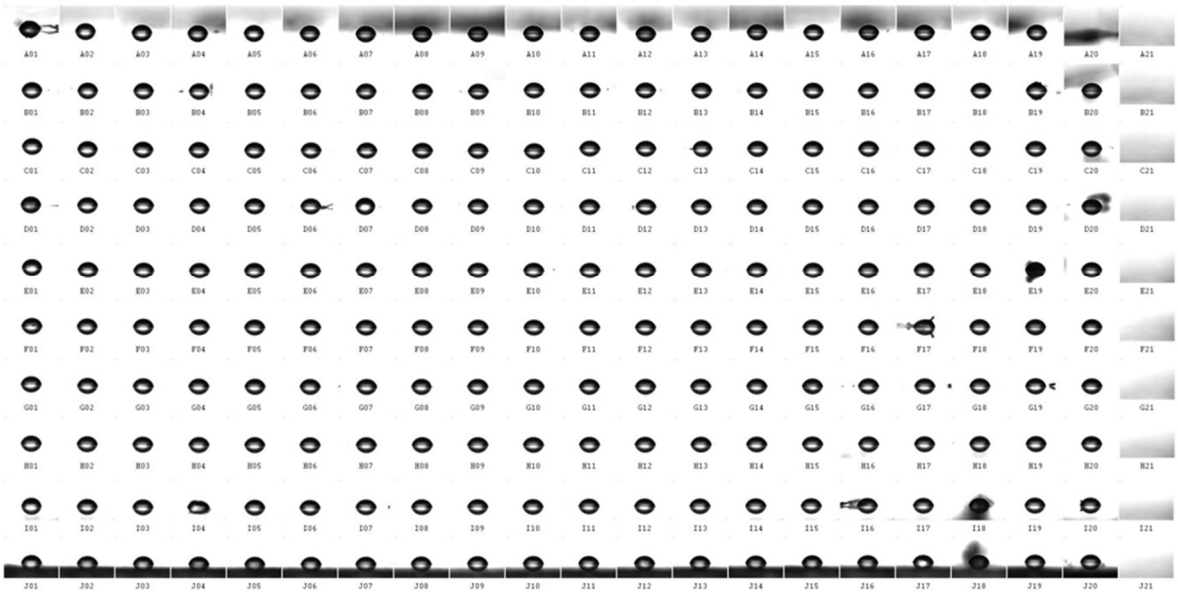

608

b) PET-*g*-PFPMA-90

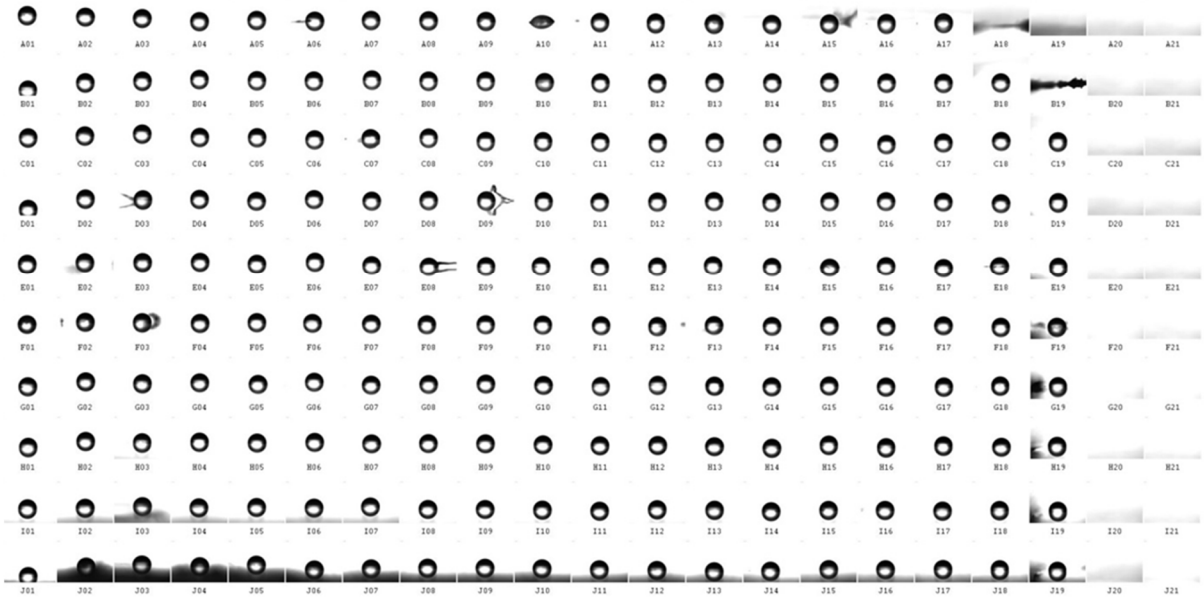

609

610 **Figure S 2. All images of 231 drops deposited on a) PET-virgin film and b) PET-*g*-PFPMA-90**

611 **film.**

Graphic Abstract

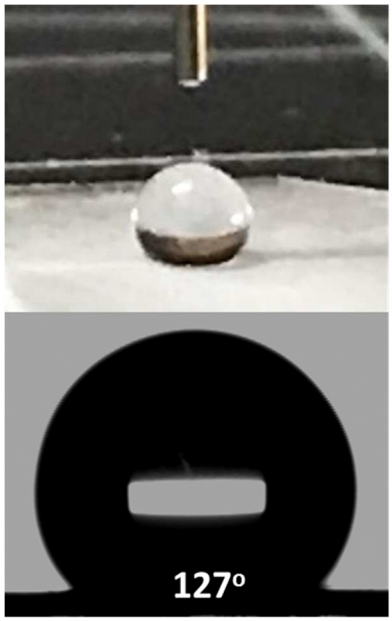

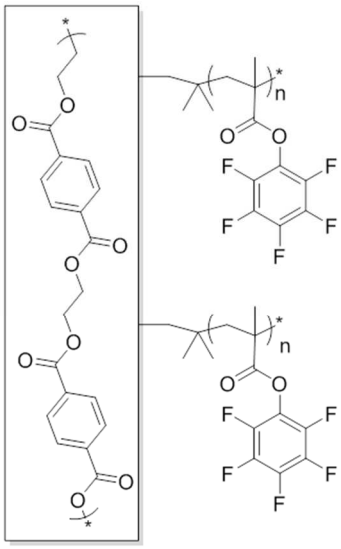

PET-pPFPMA